

# Feasibility of enhancing the thermoelectric power factor in $\text{GaN}_x\text{As}_{1-x}$

P. Pichanusakorn,<sup>1</sup> Y. J. Kuang,<sup>2</sup> C. Patel,<sup>1</sup> C. W. Tu,<sup>2</sup> and P. R. Bandaru<sup>1,2</sup>

<sup>1</sup>Materials Science Program, Department of Mechanical and Aerospace Engineering, University of California, San Diego, La Jolla, California 92093, USA

<sup>2</sup>Department of Electrical and Computer Engineering, University of California, San Diego, La Jolla, California 92093, USA

(Received 9 July 2012; published 20 August 2012)

This study was motivated by the possibility of using N resonant levels interacting with the GaAs conduction band, in  $\text{GaN}_x\text{As}_{1-x}$  ( $0 < x < 2.5\%$ ), to enhance the density of states effective mass ( $m_d$ ) and consequently the thermoelectric power factor ( $S^2\sigma$ )—where  $S$  is the Seebeck coefficient and  $\sigma$  is the electrical conductivity. However, it was observed that, compared with GaAs, the power factor was reduced in spite of a small increase in the  $m_d$ . The influences of carrier passivation and dopant type, as well as the changes in the carrier scattering mechanism, which degrades the carrier mobility, are discussed.

DOI: [10.1103/PhysRevB.86.085314](https://doi.org/10.1103/PhysRevB.86.085314)

PACS number(s): 61.72.uj, 72.20.Jv, 72.20.Pa, 81.05.Ea

## I. INTRODUCTION

An enhancement of the power factor  $S^2\sigma$ , where  $S$  is the Seebeck coefficient and  $\sigma$  is the electrical conductivity, is of much importance<sup>1</sup> in obtaining higher thermoelectric (TE) efficiency at a given temperature,  $T$ , as deduced from the figure of merit,  $ZT$  ( $=[S^2\sigma/\kappa]T$ ), especially as the thermal conductivity,  $\kappa$  seems to be reaching theoretical minimum values.<sup>2–4</sup> For materials that can be described through the Boltzmann transport equation (BTE)—which encompasses most of the commonly used TE materials<sup>5</sup>—it was previously shown<sup>6</sup> that an optimal Seebeck coefficient ( $S_{\text{opt}}$ ) exists in the range of 130–200  $\mu\text{V}/\text{K}$ . Given the narrow range of  $S$ , a much improved power factor can only be obtained through increased  $\sigma$  ( $=ne\mu$ ), implying an increased carrier (of charge  $e$ ) concentration,  $n$ , and mobility,  $\mu$ . In semiconductor-based thermoelectrics, there is typically a limit<sup>7</sup> to how much the  $n$  could be increased based on solubility limits of the dopant in the host semiconductor. However, in addition to the solubility limit, a fundamental understanding of  $n$  could be obtained by examining the expression obtained through the BTE,<sup>8</sup> i.e.,

$$n = \frac{1}{2\pi^2} \left( \frac{2k_B T m_d}{\hbar^2} \right)^{3/2} F_{1/2}(\eta) \quad (1)$$

where  $m_d$  is the density of states (DOS) effective mass,  $\eta$  is the reduced Fermi energy ( $=E_F/k_B T$ ) with the Fermi energy,  $E_F$ , reckoned from the conduction band (CB) minimum, and  $F_{j=1/2}(\eta)$  is the  $j$ th order Fermi integral (i.e.,  $F_j(\eta) = \int_0^\infty x^j / [e^{(x-\eta)} + 1] dx$ ). From the BTE,  $S$  can also be deduced:<sup>8</sup>

$$S = \mp \frac{k_B}{e} \left[ \frac{(r+5/2)F_{r+3/2}(\eta)}{(r+3/2)F_{r+1/2}(\eta)} - \eta \right] \quad (2)$$

The above implies the crucial role of the  $\eta$  and the scattering exponent,  $r$  (from the energy-dependent relaxation time,  $\tau(E)$ , approximation  $\tau(E) \sim E^r$ ) in modulating the  $S$  and the  $n$ . For example, it can be seen that as  $\eta$  is increased (decreased), an increase (decrease) of the  $n$  and a decrease (increase) of the  $S$  is obtained. Such a contrary relationship implies an optimal value for  $\eta$  for maximal power factor:  $S^2\sigma$ . However, if  $m_d$  is increased while  $\eta$  is held constant, then  $n$  would

increase while  $|S|$  remains constant. Alternatively, if  $m_d$  is increased while  $n$  is held constant,  $\eta$  would be reduced with an accompanying enhancement of  $|S|$ . Additionally, reducing  $r$  would also reduce  $|S|$ .<sup>9</sup>

We then hypothesized that a highly mismatched alloy system (HMA) such as N-doped GaAs would be a possible system to explore such dependencies and correlations. When a III–V semiconductor, such as GaAs is doped with N to form the alloy  $\text{GaN}_x\text{As}_{1-x}$ , where typically  $0 < x < 0.1$ , the isovalent N impurity substitutes for the Group V element, with a resonant energy level ( $E_N$ ) that is inside the host semiconductor CB. The interaction between  $E_N$  and the CB has the effect of (a) narrowing the host semiconductor band gap ( $E_g$ ) due to lowering of the CB edge by 0.12 eV/atomic % N,<sup>10</sup> (b) reducing the  $\mu$  due to change in scattering processes,<sup>11</sup> and (c) increasing  $m_d$ , all of which would considerably affect the electronic properties. Although the reduction in  $\mu$  is undesirable for improving the power factor, it would be interesting to investigate whether the increased  $m_d$  in N-doped GaAs could enhance  $S^2n$  as was previously observed in TI-doped PbTe.<sup>12</sup> In our investigations, we were inspired by the possibility of using N resonant levels akin to TI-resonant states interacting with the PbTe valence band (VB), which significantly increases the  $m_d$ . In this paper, we aim to indicate the modification of the power factor in HMA alloys such as  $\text{GaN}_x\text{As}_{1-x}$  through measurement and interpretation of  $S^2n$  and  $\mu$ . From a fundamental perspective, the role of the scattering mechanism, through a change of  $r$  and modulation of  $m_d$  will be discussed.

In  $\text{GaN}_x\text{As}_{1-x}$  the modification of band structure was initially described as a result of band anti-crossing (BAC<sup>13,14</sup>)—type interactions between the host GaAs CB and  $E_N$ . Such a model postulates a splitting of the CB into an *upper*  $E_+$  and a *lower*  $E_-$  subband, where the latter forms the CB minimum. As  $x$  is increased, the BAC model predicts a monotonic decrease of the CB minimum along with a concomitant increase in  $m_d$  due to a decreased band curvature. Consequently, the DOS, which is proportional to  $m_d$ , increases particularly close to  $E_N$ . Alternatively, the added N may aggregate and form *cluster* states with localized energy levels, the location of which is dependent on the N configuration within the clusters.<sup>15</sup> In the LCINS (Linear Combination of Isolated Nitrogen resonant

States) framework, such cluster states further increase  $m_d$  (in addition to an increase due to  $E_N$ ) when the cluster energy levels are resonant with the  $E_-$  band.<sup>16,17</sup> For example, when  $x = 0.5\%$  a large increase in  $m_d$  from  $0.067m_0$  ( $m_0$ : free electron mass) to  $0.150m_0$  was attributed to such cluster state resonances.<sup>16</sup> However, with increasing  $x$ , the influence of the cluster states could reduce, and  $m_d$  may be predicted by the BAC model.

A number of experiments have measured  $m_d$  in  $\text{GaN}_x\text{As}_{1-x}$ , and while most show an enhancement of  $m_d$ , there also seemed to be unclear correlations in terms of the influence of doping, as will be discussed next. A very large increase in  $m_d$  up to  $0.19m_0$  at  $x = 2\%$  was observed in undoped  $\text{GaN}_x\text{As}_{1-x}/\text{GaAs}$  quantum wells, measured via cyclotron resonance-based techniques.<sup>18</sup> On the other hand, a more moderate enhancement was observed in undoped  $\text{GaN}_x\text{As}_{1-x}$  through magneto-photoluminescence measurements<sup>16,19</sup> with a maximum  $m_d$  of  $\sim 0.15m_0$  at  $x = 1.8\%$ . On the other hand, thermoelectric technique-based measurements have instead shown a decrease in  $m_d$  to  $\sim 0.03m_0$  for Se-doped ( $n$  of  $5\text{--}7 \times 10^{18}/\text{cm}^3$ )  $\text{GaN}_x\text{As}_{1-x}$  at  $x < 0.4\%$ .<sup>20</sup> However, a recent report recorded an increase in  $m_d$  to  $\sim 0.16m_0$  for Te-doped ( $n$  of  $3\text{--}5 \times 10^{17}/\text{cm}^3$ )  $\text{GaN}_x\text{As}_{1-x}$  at  $x \sim 1.7\%$ .<sup>21</sup> Whether such differences were related to the measurement methods or due to the intrinsic material properties are difficult to understand but could yet indicate the specific influence of doping in changing  $n$ . We then seek to investigate Si-doped ( $n$ -type doping)  $\text{GaN}_x\text{As}_{1-x}$  and compare the experimental results obtained with prior literature. The aim is to understand the modification of the power factor for possible thermoelectric application.

## II. EXPERIMENTAL DETAILS

Samples of  $\text{GaN}_x\text{As}_{1-x}$  with the N composition ( $x$ ) varying in the range of 0–2.5%, were grown on semi-insulating (100) oriented GaAs substrates by gas source molecular beam epitaxy (GS-MBE). The substrate was initially heated to  $580^\circ\text{C}$  to desorb native oxide under As overpressure, and a 200-nm buffer layer of GaAs was first grown to mitigate surface roughness-related issues. The substrate temperature was then lowered to  $500^\circ\text{C}$  during the growth of the electrically active and relevant doped GaAs or  $\text{GaN}_x\text{As}_{1-x}$  layer, using 7N purity elemental Ga and thermally cracked  $\text{As}_2$  (from  $\text{AsH}_3$ ). N was injected using a 13.56-MHz nitrogen radical beam source. During the growth of the active layer, Si was incorporated through thermal evaporation from an effusion cell into the MBE chamber, with a cell temperature,  $T_{\text{Si}}$ , in the range of  $1100\text{--}1270^\circ\text{C}$ . Generally, the concentration of Si donors (i.e., [Si]) would scale with  $T_{\text{Si}}$  as:

$$[\text{Si}] \sim \exp\left(\frac{-A}{k_B T_{\text{Si}}}\right) \quad (3)$$

where  $A$  is an experimentally determined constant.<sup>22</sup> The  $x$  was maintained to be  $< 2.5\%$  for reducing the possibility of defect formation due to film–substrate lattice parameter mismatch, and it was also seen that growth with  $x < 0.5\%$  was not very reliable. The growth rate for both the buffer and active layers were  $\sim 0.2$  nm/s. The film thickness was monitored

*in situ* through reflection high-energy electron diffraction (RHEED)–based calibrations.

Subsequent to growth, the N composition ( $x$  in atomic %) was determined through the variation of the lattice constant determined by x-ray diffraction. A Vegard’s law–based interpolation between the lattice constant of GaAs (0.564 nm) and GaN (0.519 nm) was used.<sup>23</sup> Such a measurement may only account for  $N_{\text{As}}$  (such a notation indicates substitutional N on an As site) since N aggregates may not contribute to a change in the lattice constant. Through the additional use of secondary ion mass spectroscopy (SIMS)—which measures the *total* N concentration—the N aggregate concentration could be inferred by subtracting the  $N_{\text{As}}$  obtained from x-ray diffraction. However, a recent study that used both SIMS and x-ray diffraction, for the above reason, indicated that N is incorporated mostly as  $N_{\text{As}}$  for  $x < 3\%$ ,<sup>24</sup> which falls within the range of compositions studied in this work.

Carrier concentration,  $n$ , was measured by determining resistivity with the well-known van der Pauw (VDP) methodology and with Hall coefficient measurements. Figure 1 shows the arrangement used for the purpose. Ge/Ni/Au were sequentially deposited via electron beam evaporation for electrical contacts.<sup>25</sup> The contacts were annealed at  $450^\circ\text{C}$  in flowing  $\text{N}_2$  for  $\sim 5$  min in a rapid thermal annealing (RTA) chamber. Samples were placed with the active layer facing down on a sacrificial GaAs substrate during the annealing to minimize loss of As through diffusion. The GaAs and  $\text{GaN}_x\text{As}_{1-x}$  layers were patterned through plasma etching (using 10 standard cubic centimeters per minute [sccm] of  $\text{BCl}_3$  and 5 sccm of Ar (200 W, 20 mTorr), yielding an etch rate of  $\sim 1\text{--}2$  nm/s). Further processing and experimental details have been elucidated previously.<sup>26</sup>

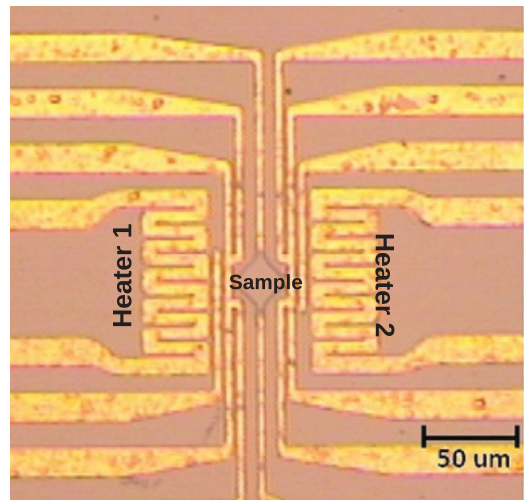


FIG. 1. (Color online) The layout of the van der Pauw arrangement for the measurement of the thermoelectric power factor ( $S^2\sigma$ ) characteristics of the  $\text{GaN}_x\text{As}_{1-x}$  samples. Four-point measurements of the electrical resistance were carried out for determining the conductivity ( $\sigma$ ) in conjunction with Hall measurements for the mobility ( $\mu$ ) and carrier concentration ( $n$ ). The heating lines/heaters for establishing a temperature gradient for the Seebeck coefficient ( $S$ ) are also indicated.

### III. RESULTS AND DISCUSSION

#### A. Compensation and passivation affects the carrier concentration, $n$

The VDP measurements indicated an increase of  $n$  with  $T_{\text{Si}}$  at any given  $x$ . However, at a given  $T_{\text{Si}}$ , samples with higher  $x$  were seen to have lower  $n$ . The underlying rationale seems to be due to passivation of the Si donors by N, and the relevant issues will be discussed later. To maintain the same  $n$  (which was in the range of  $3 \times 10^{17}/\text{cm}^3$  to  $1 \times 10^{18}/\text{cm}^3$ ) as  $x$  is increased, the  $T_{\text{Si}}$  had to be increased to compensate for such passivation. An empirical model was used to predict the required  $T_{\text{Si}}$  for MBE growth by assuming that, for samples grown at the same temperature,  $n$  scales exponentially as  $1/x$ .

The measured  $n$  was plotted as a function of the  $T_{\text{Si}}$  (see Fig. 2), from which it was observed that  $n$  increases to  $\sim 7 \times 10^{18}/\text{cm}^3$  up to a  $T_{\text{Si}} \sim 1250^\circ\text{C}$ , beyond which there is a decrease. It has been previously been reported<sup>27,28</sup> that when the concentration of Si donors (i.e.,  $[\text{Si}]$ ) exceeds  $5 \times 10^{18}/\text{cm}^3$ , the role of electron acceptor defects (e.g.,  $\text{Si}_{\text{As}}$ ), Ga vacancies, and Si clusters rapidly increases as well. Such defects compensate for electrons from the Si donors, which are normally incorporated on Ga sites (i.e., as  $\text{Si}_{\text{Ga}}$ ), leading to a decrease in  $n$ , as was indeed observed at  $T_{\text{Si}} > 1250^\circ\text{C}$ . In this regard, a compensation ratio,  $\gamma = (N_{\text{D}} + N_{\text{A}})/n$  was defined<sup>29</sup> to indicate the ratio of the concentration of fixed ionized centers to the concentration of mobile charges; here,  $N_{\text{D}}$  ( $=\text{Si}_{\text{Ga}}$ ) is the concentration of Si incorporated on Ga sites and performing as donors whereas  $N_{\text{A}}$  ( $=\text{Si}_{\text{As}}$ ) is the acceptor concentration. It was posited<sup>30</sup> that  $\gamma$  depends on relative availability of Ga and As vacancies and should be independent of  $[\text{Si}]$ . However, the formation energy of  $\text{Si}_{\text{As}}$  is lowered as  $[\text{Si}]$  is increased, and  $\gamma$  could therefore increase with  $[\text{Si}]$ .<sup>28</sup> At least one estimate<sup>27</sup> indicates that  $[\text{Si}_{\text{As}}]$  may be as large as 30% of the total  $[\text{Si}]$  at  $5 \times 10^{18}/\text{cm}^3$ , which implies a  $\gamma$  of  $\sim 2.5$ .

From Eq. (3), the  $n$  could then be described as a function of  $T_{\text{Si}}$  through:

$$n = \frac{[\text{Si}_{\text{Ga}}] + [\text{Si}_{\text{As}}]}{\gamma} = \frac{[\text{Si}]}{\gamma} = \frac{B}{\gamma} \exp\left(\frac{-A}{k_{\text{B}}T_{\text{Si}}}\right) \quad (4)$$

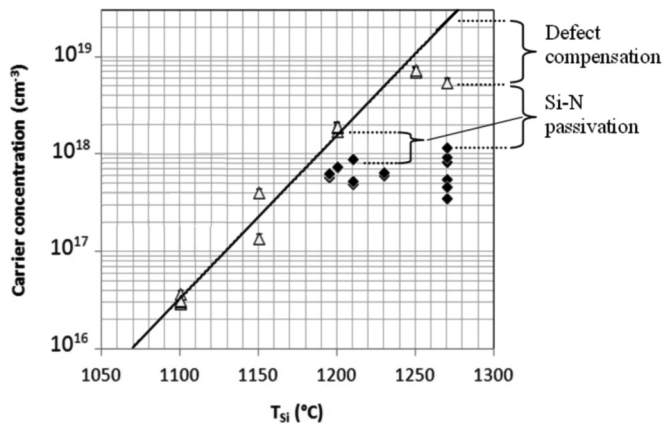


FIG. 2. The variation of the carrier concentration ( $n$ ) with  $T_{\text{Si}}$  (the Si cell temperature in the molecular beam epitaxy) for GaAs and  $\text{GaN}_x\text{As}_{1-x}$  samples, indicating the compensation and passivation regimes.

where,  $B/\gamma = 3.3 \times 10^{42}/\text{cm}^3$  and  $A = 7.1 \text{ eV}$ , as determined from the fitting of the  $n$  vs.  $T_{\text{Si}}$  data of GaAs ( $x = 0$ ) samples grown at  $T_{\text{Si}} < 1200^\circ\text{C}$ , where it is certain that  $\text{Si}_{\text{As}}$  can be the only/main source of acceptor defects. The above equation is shown as a solid line in Fig. 2. In the case of  $\text{GaN}_x\text{As}_{1-x}$ , a further decrease in  $n$  is observed that could be explained invoking Si-N mutual passivation<sup>31-34</sup> due to Coulombic interaction between the relatively positive  $\text{Si}_{\text{Ga}}$  and the relatively negative  $\text{N}_{\text{As}}$ . Unlike the long-range electron compensation due to  $\text{Si}_{\text{As}}$ , Si and N may only interact and passivate each other if they are nearest neighbors. Such Si-N interactions, which may result in  $\text{Si}_{\text{Ga}}\text{-N}_{\text{As}}$  or  $(\text{Si-N})_{\text{As}}$  (where both Si and N share a single As site) complexes, could diminish the Si donor and N concentrations. This would lead to a reduced  $n$  and if there is sufficient Si-N passivation, the band anticrossing-type energy level interactions are reduced, as were observed by the widening of the band gap back to the GaAs level.<sup>34</sup>

The extent of passivation was understood through the *doping efficiency*,  $\Phi$ , defined as the ratio of  $n$  in the  $\text{GaN}_x\text{As}_{1-x}$  to that in GaAs, both of which are grown at the same  $T_{\text{Si}}$ , i.e.,

$$\Phi = \frac{n(x, T_{\text{Si}})}{n(x=0, T_{\text{Si}})} \quad (5)$$

It was previously reported<sup>35</sup> that  $\Phi$  decreases substantially with  $T_{\text{Si}}$ , presumably due to enhanced Si-N interactions. Such a result is to be interpreted considering the relative concentrations of  $[\text{N}]$  and  $[\text{Si}]$ . For instance, at  $x = 0.5\%$ ,  $[\text{N}] \sim 2.2 \times 10^{20}/\text{cm}^3$  (given an atomic density of  $4.4 \times 10^{22}/\text{cm}^3$  for GaAs), whereas from Eq. (4) and Fig. 2,  $[\text{Si}]$  would be on the order of  $\gamma \times 10^{19}/\text{cm}^3$ . Because  $\gamma$  is not expected<sup>29</sup> to be greater than  $\sim 10$ —also see Fig. 3—the addition of Si would not affect the doping efficiency much because Si-N passivation demands near-neighbor interactions, and modulation of  $\Phi$  implies that Si be in proximity to N, which is improbable through MBE-based evaporation. Indeed, Si-N passivation in  $\text{GaN}_x\text{As}_{1-x}$  was not observed when Si was introduced via ion-implantation; passivation was only evidenced after annealing at  $T > 600^\circ\text{C}$  for  $t = 10 \text{ s}$ , when the diffusion length,  $L_{\text{D}} (= \sqrt{D_{\text{Si}}t})$ , where  $D_{\text{Si}}$  is the diffusivity of Si in GaAs<sup>36</sup> was comparable to the average separation, i.e.,  $L_{\text{N}} (= \sqrt[3]{[\text{N}]})$ , between the N atoms.<sup>34</sup>

In this context, the samples in our study were subject to two heating cycles; i.e., (1) during growth where substrate was held at  $500^\circ\text{C}$  for  $\sim 1000 \text{ s}$  of active layer deposition (200 nm at 0.2 nm/s) and (2) during contact annealing at  $450^\circ\text{C}$  for 300 s. Using the previously quoted  $D_{\text{Si}}$  value,  $L_{\text{D}}$  was calculated to be 0.07 nm and 0.01 nm for the two steps, respectively. For an  $x \sim 0.5 - 2.5\%$ , the  $L_{\text{N}}$  is approximately in the range of 1.0–1.6 nm. Therefore, bulk diffusion should not be sufficient. However, to explain the extensive passivation in our studies and that of others,<sup>33</sup> it was necessary to speculate that surface diffusivity of Si adatoms is higher than that of Si diffusivity in the bulk. Additional enhancement of Si surface diffusion may occur through Coulombic attraction. Considering the Debye length ( $\lambda_{\text{D}}$ ) as a metric for charge interactions and from  $\lambda_{\text{D}} = \sqrt{(\epsilon_0 \epsilon_r k_{\text{B}} T)/e^2 n}$ , where  $\epsilon_0$  is the permittivity of free space,  $\epsilon_r$  is the relative static permittivity of GaAs ( $=13.1$ ), and  $n \sim (3-10) \times 10^{17}/\text{cm}^3$  at  $T = 300 \text{ K}$ , a  $\lambda_{\text{D}}$  in the range of 4–7 nm

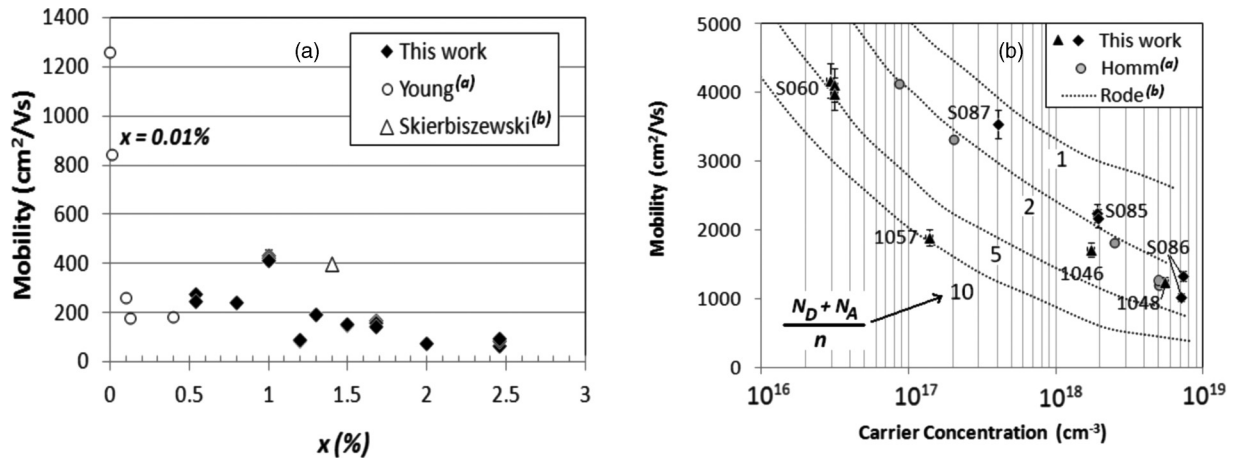


FIG. 3. (a) The variation of the carrier mobility ( $\mu$ ) of  $n$ - $\text{GaN}_x\text{As}_{1-x}$  as a function of N composition. The comparison of our data to that of (a) Young *et al.* (see Ref. 20) and (b) Skierbiszewski *et al.* (see Ref. 47) is indicated. (b) A comparative variation of the carrier mobility ( $\mu$ ) of  $n$ -GaAs with carrier concentration compared with that of a representative study from literature, i.e., (a) Homm *et al.* (see Ref. 48). The dashed lines were adapted from the prior calculations of (b) Rode *et al.* (see Ref. 29).

was calculated. Since  $\lambda_D > L_N$ , it would now be expected that Coulombic forces between N and Si would need to be considered for Si-N passivation.

**B. Decreased carrier mobility,  $\mu$ , in  $\text{GaN}_x\text{As}_{1-x}$**

The  $\mu$  was found to be significantly decreased by the addition of N (i.e., increasing  $x$  in  $\text{GaN}_x\text{As}_{1-x}$ )—see Fig. 3(a). Additionally, N complexes may also be a significant source of scattering.<sup>11</sup> The sharp reduction below  $x = 0.1\%$  is in accord with previous reports<sup>20</sup> and is indicative of a sudden change in scattering mechanism, whereas the more gradual decrease above  $x = 0.1\%$  may be due to an increase of both [N] and [Si]. However, because  $[\text{N}] \gg [\text{Si}]$ ,  $\mu$  should be largely independent of  $n$  or [Si]. The reduction in  $\mu$  then occurs due to (a) an increase in the  $m_d$  as previously considered, by invoking the BAC model, and (b) due to increased *alloy-like* scattering because of  $\text{N}^{37}$  compared with the native As.<sup>38,39</sup>

For comparison, we also plot the variation of  $\mu$  with  $n$  for GaAs, superposed on which are the contours of constant  $\gamma$ , obtained using previous calculations.<sup>29</sup> An increase in  $\gamma$  could indicate a strong onset of compensation through moieties such as  $\text{Si}_{\text{As}}$ , Ga vacancies, Si clusters, etc. The observation of increasing  $\gamma$  with  $n$  is in accordance with the data of Fig. 2. Generally, a high  $\gamma$  (e.g.,  $\sim 5$ – $10$ ) observed for some samples, e.g., S060 and 1057 in Fig. 3(b), likely indicates substantial defect formation and may be used as a guide for growth optimization.

**C. Reduction of the Seebeck coefficient,  $S$**

The Seebeck coefficient ( $S$ ) of  $\text{GaN}_x\text{As}_{1-x}$  was measured as a function of  $x$  and is shown in Fig. 4(a). To verify the accuracy of our measurements, the  $S$  of GaAs was measured as well and compared with literature values, as indicated in Fig. 4(b). A good fit between the calculation and measurement was found for  $r = 0.26$ , as suggested through previous Nernst coefficient values.<sup>20</sup> Our calculations also considered the increase in  $m_d$  with  $n$  due to GaAs CB non-parabolicity.<sup>40</sup>

The dominant scattering mechanism in GaAs is considered to be polar optical phonon (POP) scattering,<sup>39</sup> which cannot be accurately represented by the simple power law of the form  $\tau(E) \sim E^r$ . However, the scattering rate of POP has different constant values above and below 0.05 eV and a characteristic  $r \sim 0$  for the POP processes may be assumed.<sup>41</sup> The lower  $S$  measured for the samples with  $n \sim 3 \times 10^{16}/\text{cm}^3$  in Fig. 4(b) may be due to higher impurity concentration, as also indicated by the higher  $\gamma$ —see Fig. 3(b). If  $n$  is high enough, the increased impurity concentration could strengthen strongly screened ionized scattering, which could explain why the  $S$  values for such samples are modeled as closer to  $r = -1/2$ . On the contrary, if  $n$  is low, then weakly screened Coulomb scattering could be promoted (with  $r = 3/2$ ) and  $S$  would be increased instead (as can also be seen through Eq. (2)). Other calculations<sup>29</sup> also suggest an increase in  $S$  with  $\gamma$ , presumably because of the latter type of scattering.<sup>41</sup>

For  $\text{GaN}_x\text{As}_{1-x}$ , the relationship between  $S$  and  $x$ , as in Fig. 4(a), is not clear since  $n$  still varies for most samples and  $S$  decreases with increasing  $n$ . To highlight the trend, data points for samples with  $n$  closest to the average value of  $4 \times 10^{17}/\text{cm}^3$  are indicated (as black data points) in this figure, from which it was observed that  $S$  seems to have a minimum at  $x \sim 1\%$ . It was generally seen that the  $S$  for  $\text{GaN}_x\text{As}_{1-x}$  was lower than that for GaAs for all the investigated N compositions. However, the variation in  $n$  may affect such a comparison because the GaAs sample has the lowest  $n$  ( $\sim 3 \times 10^{17}/\text{cm}^3$ ). Therefore, the product  $S^2n$  is indicated in Fig. 5. A minimum at  $x \sim 1\%$  was again observed. While such a comparison still showed no enhancement of the  $S^2n$  product for  $\text{GaN}_x\text{As}_{1-x}$  over GaAs, the differences are much smaller. If  $n$  were actually equal, then this figure might suggest that the  $S$  of  $\text{GaN}_x\text{As}_{1-x}$  is, at most, comparable to that of GaAs. The general decrease in  $S^2n$  may be due to a change in scattering mechanism. The addition of N is responsible for a large decrease in  $\mu$  through a change from POP to alloy scattering. A decrease of  $r$  by  $1/2$  can reduce  $S$  by approximately  $30$ – $50 \mu\text{V}/\text{K}$ .<sup>8</sup> However, there may yet be an enhancement in  $m_d$ .

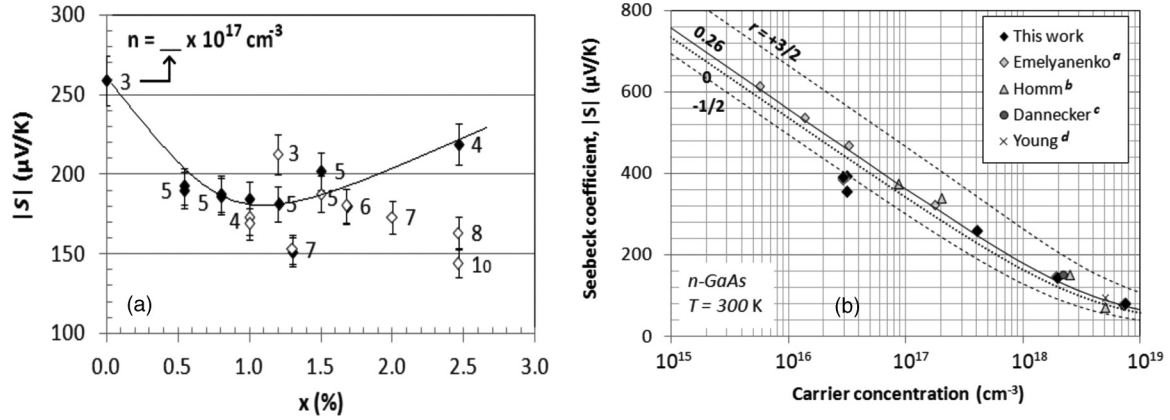


FIG. 4. (a) The Seebeck coefficient ( $S$ ) of Si-doped  $\text{GaN}_x\text{As}_{1-x}$  as a function of N composition ( $x$ ). (b) The  $S$  vs carrier concentration ( $n$ ) of  $n$ -GaAs as measured in this work and compared with that of (a) Emelyanenko *et al.* (see Ref. 49), (b) Homm *et al.* (see Ref. 48), (c) Dannecker *et al.* (see Ref. 21), and (d) Young *et al.* (see Ref. 20). The analytical calculation assuming various  $r$  values are indicated through lines.

#### D. Enhancement of the effective mass, $m_d$ , due to N addition

The DOS effective mass ( $m_d$ ) was calculated from the measured  $S$  and  $n$  as follows:

(1) Given a pair of ( $S, n$ ),  $\eta$  was first numerically interpolated from Eq. (2); whereas  $r = 0.26$  was assumed for GaAs,  $r = -1/2$  for  $\text{GaN}_x\text{As}_{1-x}$ , as discussed in the previous section.

(2) The  $m_d$  was estimated from  $m_d = \frac{\pi\hbar^2}{k_B T} \left( \frac{2^{1/2} N_o}{N_c} \right)^{2/3}$ , where  $N_o = \frac{n_i}{F_{1/2}(\eta)} \left( \frac{\pi}{4} \right)^{1/2}$  and the number of conduction band valleys/degeneracy,  $N_c$ , was 1.

Many issues had to be carefully considered for the above estimation; e.g., the temperature during the  $S$  measurement was typically  $\sim 10^\circ\text{C}$  higher than that during the  $n$  measurement because of Joule heating required to provide a temperature difference in the former. In our calculations, the  $T$  in the  $S$  measurement was used, but if a lower  $T$  (as measured during  $n$ ) is used, then  $m_d$  would have increased by  $\sim 3\%$ . However, a more significant source of error was the assumption of an appropriate  $r$  value. Figure 6 shows the values of  $m_d$  that were estimated from our measurements compared with the values from literature. Where not explicitly stated, we estimated the  $r$  values from prior experimental data<sup>20</sup> and formulae,<sup>42</sup> which indicated that  $r \sim 0.26$  for GaAs and decreases to about  $-0.6$

for  $\text{GaN}_x\text{As}_{1-x}$  (with  $x = 0.4\%$ ). The transition to a negative  $r$  for  $\text{GaN}_x\text{As}_{1-x}$  is consistent with the earlier discussion and justifies the use of the above  $r$ .

While Dannecker *et al.*<sup>21</sup> used  $r = -1/2$  for  $\text{GaN}_x\text{As}_{1-x}$ , an  $r = 3/2$  was chosen by their group for GaAs (which resulted in a lower  $m_d$  for GaAs of  $\sim 0.048m_e$ , compared with  $\sim 0.072m_e$  in our case, despite similar  $S$  and  $n$ , as in Fig. 3(b)) on the basis that (weakly screened) ionized impurity scattering should dominate for doped samples.<sup>29</sup> However, calculations<sup>39</sup> suggest that POP scattering should be more dominant near room temperature; additionally, the compilation of  $S$ - $n$  data for GaAs in Fig. 4(b) does support a smaller  $r$  of  $\sim 0.26$ . On the other hand, Young *et al.*<sup>20</sup> observed a strong decrease in  $m_d$  attributed to the narrowing of band gap ( $E_g$ ) in accordance

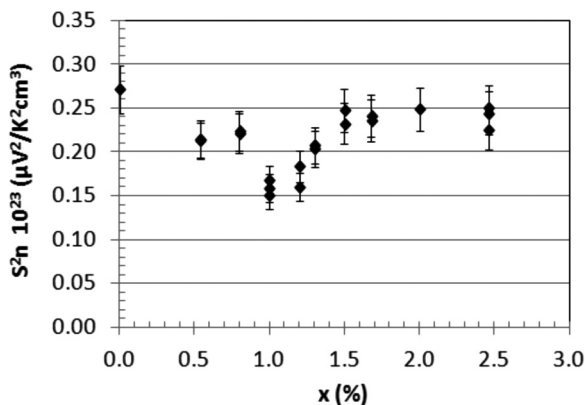


FIG. 5. The variation of  $S^2 n$  of Si-doped  $\text{GaN}_x\text{As}_{1-x}$  as a function of N composition ( $x$ ).

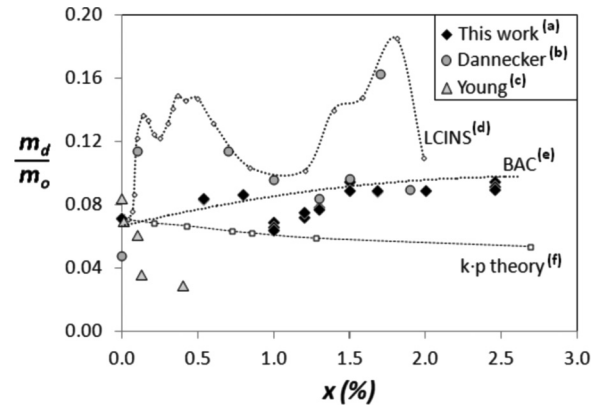


FIG. 6. The density of states effective mass ( $m_d$ ) as a fraction of the bare electron effective mass ( $m_o$ ) comparing three types of dopant, (a) Si,  $n \sim (3-10) \times 10^{17}/\text{cm}^3$ , as in this work; (b) Te,  $n \sim (3-5) \times 10^{17}/\text{cm}^3$  from Dannecker *et al.* (see Ref. 21<sup>21</sup>); and (c) Se,  $n \sim (5-7) \times 10^{18}/\text{cm}^3$  from Young *et al.* (see Ref. 20<sup>20</sup>). Theoretical models were reproduced from earlier work, e.g., the (d) LCINS model by Masia *et al.* (see Ref. 16), (e) BAC model by Shan *et al.* (see Ref. 13), and (f) k-p model by Katsuhiko *et al.* (see Ref. 10). The error bar for our data is small and invisible at this scale, whereas for data from Dannecker *et al.*, the error bars ( $\pm 0.019$ ) were omitted for clarity.

with k-p theory<sup>43</sup> where  $m_d$  was estimated through:

$$\frac{m_d}{m_o} = \frac{m_o E_g}{2P^2} \approx \frac{E_g}{20eV} \quad (6)$$

Here,  $P^2$  is a matrix element<sup>43</sup> between the electron wavefunctions (similar for most III–V and II–VI semiconductors). The calculated  $m_d$  was then plotted as in Fig. 6, where the reduction of  $m_d$  as predicted by k-p theory was found to be much less than that observed by Young *et al.*<sup>20</sup> On the contrary, Dannecker *et al.*<sup>21</sup> observed a drastic increase with large fluctuations in  $m_d$  that appear to follow the LCINS model. As the figure shows, at least two characteristic peaks (at  $x \sim 0.4\%$  and  $x \sim 0.5\%$ ) were predicted by the LCINS model and attributed to the contribution from the cluster states of N-Ga-N and N-Ga-N-Ga-N chains,<sup>16</sup> respectively. In the absence of effective, interacting cluster states (e.g., at  $x \sim 1\%$ ),  $m_d$  reverts to the BAC model predicted levels.

In the present work, we observe an increase in  $m_d$  that is more in agreement with the BAC model.<sup>13</sup> However, the observation of a local minimum at  $x \sim 1\%$ , which coincides with results from both Dannecker *et al.*<sup>21</sup> and the LCINS model, was puzzling. While the absence of a peak at  $x$  of 0.3%, 0.5%, or 1.7% could be due to the absence of effective N aggregates, a decrease of  $m_d$  below the level predicted by the BAC model is unexpected since  $E_N$  should always be present. It was worth noting that the reduction was close to the level predicted by k-p theory, which may indicate that the band gap reduction could indeed affect the  $m_d$  for  $\text{GaN}_x\text{As}_{1-x}$ .

The absence of contribution from N aggregates may be related to the use of different dopant species in each experiment. While the samples in our study were Si doped, those of Dannecker *et al.*<sup>21</sup> and Young *et al.*<sup>20</sup> were doped with Te and Se, respectively. While Si may be incorporated into both Ga and As lattice sites, Te and Se would be solely substituting for As. Consequently, amphoteric defect compensation is absent in Te- or Se-doped GaAs. However, Ga vacancy defects still arise as [Te] is increased, which similarly limits  $n$  in GaAs.<sup>44</sup> Furthermore, Te and Se also cannot mutually passivate N, which also only substitutes for As (although Te and Se may be attracted to N through Coulombic forces, they cannot form a direct bond to N because As sites

are necessarily separated by Ga sites<sup>44</sup>). It is then possible to deduce, through our experiments, that Si may interact and bond with N aggregates and is a possible source of the large increase in  $m_d$ , as predicted through the LCINS model. While passivation has been described, hitherto, in terms of bonding of single  $\text{Si}_{\text{Ga}}$  to single  $\text{N}_{\text{As}}$ , it is conceivable that Si could also replace Ga in N clusters (e.g., N-Ga-N) as well. The passivation of such aggregates could prevent an increase in  $m_d$ . However, considering that the concentration of such N aggregates could only be a small fraction of the incorporated N,<sup>15</sup> and since [N] is still much greater than [Si], the overall increase in  $m_d$  would be due to BAC-like models.

#### IV. CONCLUSIONS

We began with the hypothesis that the interaction between N resonant energy level and the GaAs CB could introduce a large increase in  $m_d$  and consequently enhance the thermoelectric power factor. To test this hypothesis, the  $\sigma$  and  $S$  of Si-doped  $\text{GaN}_x\text{As}_{1-x}$  thin films with  $n \sim 3 \times 10^{17}/\text{cm}^3$  and  $0.5\% < x < 2.5\%$  were measured. While it was found that  $m_d$  was indeed increased in accordance with the established BAC model, an enhancement in  $S^2n$  compared with GaAs was not found due to a change in scattering mechanism in  $\text{GaN}_x\text{As}_{1-x}$ , which may counteract the increase in  $m_d$  and degrade the  $\mu$  as well. Therefore, one may conclude that the investigated  $\text{GaN}_x\text{As}_{1-x}$  might not be a viable thermoelectric material. However, a comparison of ion-implanted Si-doped  $\text{GaN}_x\text{As}_{1-x}$ —where the effects of Si-N passivation could be reduced and which should then show an increased  $m_d$  and  $S$ , as predicted by the LCINS model—with the results of this work would be necessary to verify such a conclusion. Additionally, other variants where Bi is used instead of N with GaAs (the Bi energy level is now resonant with the GaAs VB<sup>45</sup>) could also be studied for an enhanced power factor, in that the hole carrier mobility in such materials was shown to be reduced to a much smaller extent.<sup>46</sup>

#### ACKNOWLEDGMENTS

We gratefully acknowledge support from the National Science Foundation (Grant No. ECS-05-08514).

<sup>1</sup>P. Pichanusakorn and P. R. Bandaru, *J. Appl. Phys.* **107**, 074304 (2010).

<sup>2</sup>M. V. Simkin and G. D. Mahan, *Phys. Rev. Lett.* **84**, 927 (2000).

<sup>3</sup>D. G. Cahill, W. K. Ford, K. E. Goodson, G. D. Mahan, A. Majumdar, H. J. Maris, R. Merlin, and S. R. Phillpot, *J. Appl. Phys.* **93**, 793 (2003).

<sup>4</sup>D. G. Cahill, S. K. Watson, and R. O. Pohl, *Phys. Rev. B* **46**, 6131 (1992).

<sup>5</sup>D. M. Rowe, editor, *Thermoelectrics Handbook: Macro to Nano* (CRC Press, Boca Raton, FL, 2006).

<sup>6</sup>P. Pichanusakorn and P. R. Bandaru, *Appl. Phys. Lett.* **94**, 223108 (2009).

<sup>7</sup>W. Walukiewicz, *Physica B* **302–303**, 123 (2001).

<sup>8</sup>P. Pichanusakorn and P. R. Bandaru, *Mater. Sci. Eng., R* **67**, 19 (2010).

<sup>9</sup>P. Pichanusakorn and P. Bandaru, *Appl. Phys. Lett.* **94**, 223108 (2009).

<sup>10</sup>U. Katsuhiko, M. Nobuki, and S. Ikuo, *Appl. Phys. Lett.* **74**, 1254 (1999).

<sup>11</sup>S. Fahy and E. P. O'Reilly, *Physica E: Low-dimensional Systems and Nanostructures* **21**, 881 (2004).

<sup>12</sup>J. P. Heremans, V. Jovovic, E. S. Toberer, A. Saramat, K. Kurosaki, A. Charoenphakdee, S. Yamanaka, and G. J. Snyder, *Science* **321**, 554 (2008).

<sup>13</sup>W. Shan, W. Walukiewicz, J. W. Ager, E. E. Haller, J. F. Geisz, D. J. Friedman, J. M. Olson, and S. R. Kurtz, *Phys. Rev. Lett.* **82**, 1221 (1999).

- <sup>14</sup>T. Mattila, S.-H. Wei, and A. Zunger, *Phys. Rev. B* **60**, R11245 (1999).
- <sup>15</sup>P. R. C. Kent and A. Zunger, *Phys. Rev. B* **64**, 115208 (2001).
- <sup>16</sup>F. Masia, G. Pettinari, A. Polimeni, M. Felici, A. Miriametro, M. Capizzi, A. Lindsay, S. B. Healy, E. P. O'Reilly, A. Cristofoli, G. Bais, M. Piccin, S. Rubini, F. Martelli, A. Franciosi, P. J. Klar, K. Volz, and W. Stolz, *Phys. Rev. B* **73**, 073201 (2006).
- <sup>17</sup>A. Lindsay and E. P. O'Reilly, *Phys. Rev. Lett.* **93**, 196402 (2004).
- <sup>18</sup>P. N. Hai, W. M. Chen, I. A. Buyanova, H. P. Xin, and C. W. Tu, *Appl. Phys. Lett.* **77**, 1843 (2000).
- <sup>19</sup>F. Masia, A. Polimeni, G. Baldassarri, H. von Hogerthal, M. Bissiri, M. Capizzi, P. J. Klar, and W. Stolz, *Appl. Phys. Lett.* **82**, 4474 (2003).
- <sup>20</sup>D. L. Young, J. F. Geisz, and T. J. Coutts, *Appl. Phys. Lett.* **82**, 1236 (2003).
- <sup>21</sup>T. Dannecker, Y. Jin, H. Cheng, C. F. Gorman, J. Buckeridge, C. Uher, S. Fahy, C. Kurdak, and R. S. Goldman, *Phys. Rev. B* **82**, 125203 (2010).
- <sup>22</sup>T. Tomooka, Y. Shoji, and T. Matsui, *J. Mass Spectrom. Soc. Jpn.* **47**, 49 (1999).
- <sup>23</sup>W. G. Bi, F. Deng, S. S. Lau, and C. W. Tu, *J. Vac. Sci. Technol. B* **13**, 754 (1995).
- <sup>24</sup>W. J. Fan, S. F. Yoon, T. K. Ng, S. Z. Wang, W. K. Loke, R. Liu, and A. Wee, *Appl. Phys. Lett.* **80**, 4136 (2002).
- <sup>25</sup>M. Heiblum, M. I. Nathan, and C. A. Chang, *Solid State Electron.* **25**, 185 (1982).
- <sup>26</sup>P. Pichanusakorn, Ph.D. thesis, University of California, San Diego, 2012.
- <sup>27</sup>S. Schuppler, D. L. Adler, L. N. Pfeiffer, K. W. West, E. E. Chaban, and P. H. Citrin, *Appl. Phys. Lett.* **63**, 2357 (1993).
- <sup>28</sup>C. Domke, P. Ebert, M. Heinrich, and K. Urban, *Phys. Rev. B* **54**, 10288 (1996).
- <sup>29</sup>D. L. Rode and S. Knight, *Phys. Rev. B* **3**, 2534 (1971).
- <sup>30</sup>Y. G. Chai, R. Chow, and C. E. C. Wood, *Appl. Phys. Lett.* **39**, 800 (1981).
- <sup>31</sup>J. Li, P. Carrier, S.-H. Wei, S.-S. Li, and J.-B. Xia, *Phys. Rev. Lett.* **96**, 035505 (2006).
- <sup>32</sup>A. Janotti, P. Reunchan, S. Limpijumngong, and C. G. Van de Walle, *Phys. Rev. Lett.* **100**, 045505 (2008).
- <sup>33</sup>Y. Jin, Y. He, H. Cheng, R. M. Jock, T. Dannecker, M. Reason, A. M. Mintairov, C. Kurdak, J. L. Merz, and R. S. Goldman., *Appl. Phys. Lett.* **95**, 092109 (2009).
- <sup>34</sup>K. M. Yu, W. Walukiewicz, J. Wu, D. E. Mars, D. R. Chamberlin, M. A. Scarpulla, O. D. Dubon, and J. F. Geisz, *Nat. Mater.* **1**, 185 (2002).
- <sup>35</sup>P. Pichanusakorn, Y. J. Kuang, C. J. Patel, C. W. Tu, and P. R. Bandaru, *Appl. Phys. Lett.* **99**, 072114 (2011).
- <sup>36</sup>E. F. Schubert, J. B. Stark, T. H. Chiu, and B. Tell, *Appl. Phys. Lett.* **53**, 293 (1988).
- <sup>37</sup>S. Fahy, A. Lindsay, H. Ouerdane, and E. P. O'Reilly, *Phys. Rev. B* **74**, 035203 (2006).
- <sup>38</sup>M. P. Vaughan and B. K. Ridley, *Phys. Rev. B* **75**, 195205 (2007).
- <sup>39</sup>M. P. Vaughan and B. K. Ridley, in *Dilute III-V Nitride Semiconductors and Material Systems*, edited by A. Erol (Springer-Verlag, Heidelberg, 2008), Vol. 105, p. 255.
- <sup>40</sup>A. Raymond, J. L. Robert, and C. Bernard, *J. Phys. C* **12**, 2289 (1979).
- <sup>41</sup>M. Lundstrom, *Fundamentals of Carrier Transport* (Cambridge University Press, Cambridge, UK, 2000).
- <sup>42</sup>D. L. Young, T. J. Coutts, and V. I. Kaydanov, *Rev. Sci. Instrum.* **71**, 462 (2000).
- <sup>43</sup>P. Yu and M. Cardona, *Fundamentals of Semiconductors: Physics and Material Properties* (Springer, New York, 2005).
- <sup>44</sup>J. Gebauer, E. R. Weber, N. D. Jager, K. Urban, and P. Ebert, *Appl. Phys. Lett.* **82**, 2059 (2003).
- <sup>45</sup>S. Francoeur, M. J. Seong, A. Mascarenhas, S. Tixier, M. Adamcyk, and T. Tiedje, *Appl. Phys. Lett.* **82**, 3874 (2003).
- <sup>46</sup>D. A. Beaton, R. B. Lewis, M. Masnadi-Shirazi, and T. Tiedje, *J. Appl. Phys.* **108**, 083708 (2010).
- <sup>47</sup>C. Skierbiszewski, P. Perlin, P. Wisniewski, T. Suski, W. Walukiewicz, W. Shan, J. W. Ager, E. E. Haller, J. F. Geisz, D. J. Friedman, J. M. Olson, and S. R. Kurtz, *Phys. Stat. Sol. (B)* **216**, 135 (1999).
- <sup>48</sup>G. Homm, P. J. Klar, J. Teubert, W. Heimbrodt, *Appl. Phys. Lett.* **93**, 042107 (2008).
- <sup>49</sup>O. V. Emelyanenko, D. N. Nasledov, V. G. Sidorov, V. A. Skripkin, and G. N. Talalakin, *Phys. Stat. Sol. B* **12**, K93 (1965).